Engineering Research Express

PAPER

Multi-impact response of CR4 mild steel: characterising the transition from absorption to failure

B Thawani, T Batchelor, J Painter, R Hazael* and R Critchley

Cranfield Forensic Institute, Cranfield University, Defence Academy of the United Kingdom, Shrivenham SN6 8LA, United Kingdom

* Author to whom any correspondence should be addressed.

E-mail: rachael.hazael@cranfield.ac.uk

Keywords: petalling, ballistic, energy absorption, CR4 mild steel, impact response

OPEN ACCESS

RECEIVED
1 December 2022

REVISED
1 March 2023

ACCEPTED FOR PUBLICATION
2 March 2023

PUBLISHED
15 March 2023

Original content from this work may be used under the terms of the Creative Commons Attribution 4.0 licence.

Any further distribution of this work must maintain attribution to the author(s) and the title of the work, journal citation and DOI.

Abstract

Single impact perforation shots are well understood for various target materials and different shaped projectiles. Although considered a rare case, localised multi-impacts are not well understood as they involve both perforating and non-perforating impacts on the target. The lack of understanding of non-perforating impact on metallic materials makes it tough to predict the change in the material's mechanical performance. Given the widespread use of metallic materials for protective applications, it is important to understand the material response when subject to multiple impacts. To determine the effect of a non-perforating shot on CR4 mild steel and establish a minimum energy impact that will define the transition point whereby the metal can no longer absorb energy a series of impact experiments were conducted. Results show a subsequent perforation event occurs at a lower than the experimentally determined perforation velocity. Results suggest that there could be a direct correlation between the material thickness and the critical crater depth (the depth of crater required to affect the materials ability to absorb energy, the measure of materials performance). As the crater depth increased from 3 mm to 8.5 mm for the first shot, the energy absorption of the steel plate reduced by 25%. This allowed the residual performance for CR4 mild steel to be quantified for a known impact crater, giving a 7% performance loss for every millimetre the critical crater depth grows beyond 3 mm until the point of failure.

Introduction

In many industries such as automotive, aerospace and security, non-perforating impacts on metallic materials are of increasing interest [1]. Where structural integrity is paramount to safety, understanding how an impact effects the materials ability to provide its intended mechanical strength is vital.

Automotive vehicles encounter multi-impact scenarios in a variety of operational roles with the most extreme example being defence and security vehicles operating as personnel carriers, reconnaissance vehicles or armoured fighting vehicles. During operations they are exposed to a multitude of threats; from road debris, small arms threats, or Improvised Explosive Devices (IEDs). These threats can often be associated with catastrophic damage to vehicles, leading to firepower, mobility or catastrophic kills [2]. Vehicles, specifically those used in military operations, the outer skin is designed to defeat incoming projectile threats by absorbing the kinetic energy of a given projectile. The majority of vehicles in these roles are constructed from metals and their alloys most commonly steel and aluminium [3]. Metals have been the preferred choice for many years, due to their desirable mechanical properties, price and workability [4, 5].

Metallic materials are well understood, and there is extensive research into their responses and failure mechanisms to single impacts with varying parameters, such as projectile geometry, target material and thickness and the velocity regime [6–10]. Impacts can be characterised in various ways, such as; the projectile or target characteristics (geometry and material type), or the impact velocity [1]. Impacts that occur below 1000 m s^{-1} have their failure modes govern by the material properties of both target and impactor. These failure

© 2023 The Author(s). Published by IOP Publishing Ltd

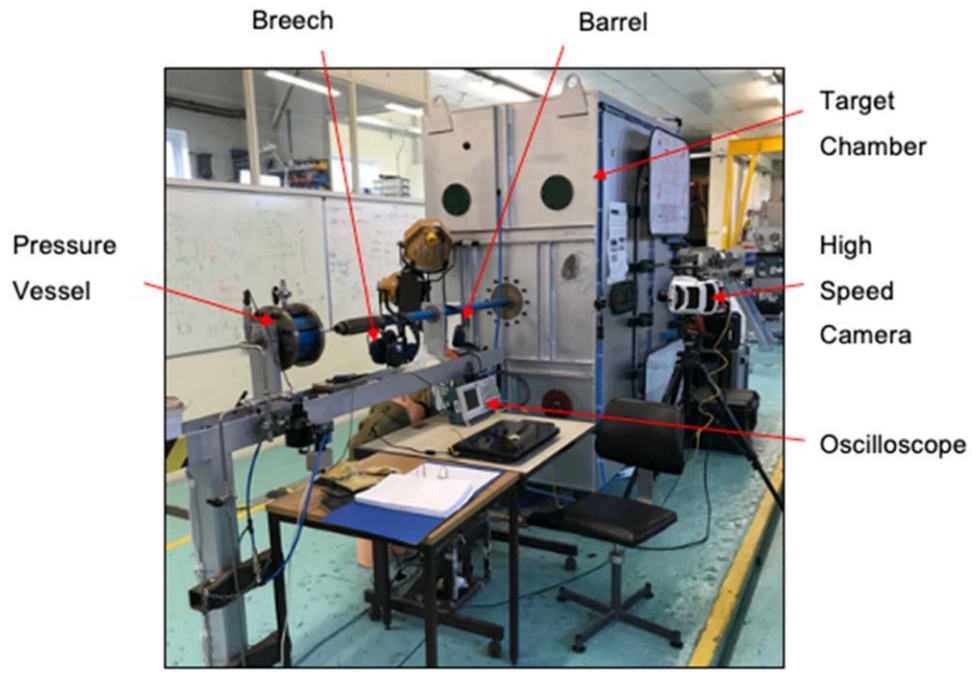


Figure 1. Single stage gas gun overview highlighting the experiment setup including high speed camera and oscilloscope to measure impact velocity and error.

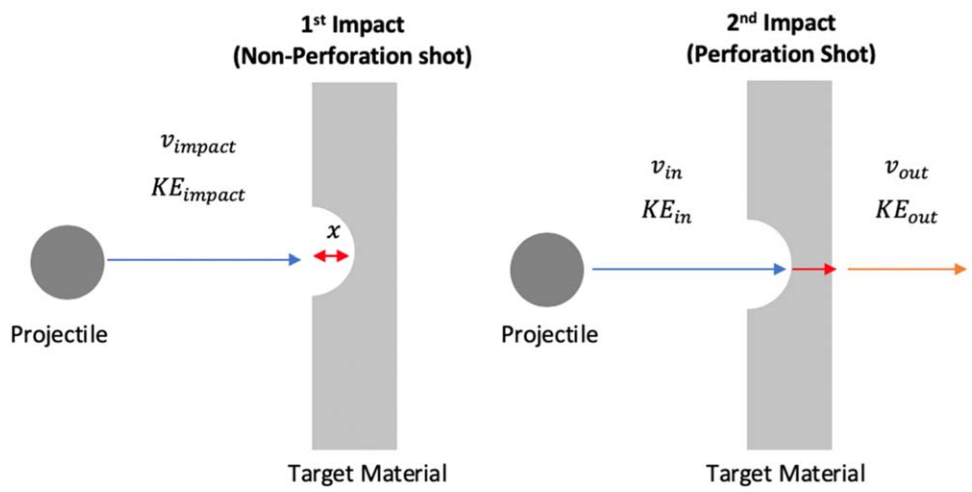


Figure 2. The multi-impact process; measured variables (impact velocity of projectile; crater depth; exit velocity of projectile); and calculated variables (kinetic energy of projectile during impact; and kinetic energy of projectile after perforation).

mechanisms are extensively discussed throughout literature, are well understood [1, 7, 11–14] and have highlighted the most common failure mechanisms experienced to be petalling and plugging. Petalling is produced by the high radial tensile stresses generated near the lip of the projectile, while plugging is due to the high shear forces generate by the projectile during perforation [11]. Projectile impacts can produce a variety of effects. These varying effects are credited to projectile and material properties, such as hardness, strength, ductility and the relative velocity of the colliding target and projectile [9, 15, 16]. In the lowest range of impact velocities the material behaviour would be expected to be elastic (with no permanent plastic deformation) [1, 9]. As the impact velocity increases, a ductile target is likely to experience an increasing amount of plastic flow (permanent deformation), whilst a brittle target will experience shattering or fragmentation as its failure mode. As the projectile velocity continues to increase the increasing amount of plastic deformation in a ductile plate converts into perforation of the target. Prominent research has been conducted on the topic of material response when subject to different kinds of projectile impact. This research has been focused around the shape and velocity of the projectiles; different target materials; and empirical studies of the different failure modes [7, 8, 15–24]. Besides the visual damage seen post projectile impact which is extensively covered in current literature,

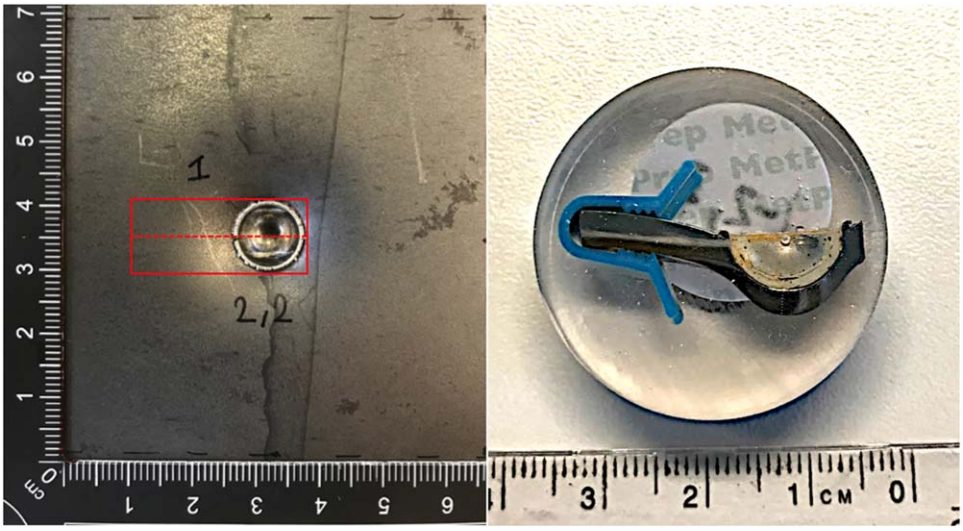


Figure 3. Impact crater sample outlining the cuts made for hardness test sample (left); prepared sample ready for Vickers hardness test to observe change in material properties (right).

the effect on the material's mechanical response post impact is not understood. For example, if a multi-hit scenario were to occur on a vehicle, and the impacted metallic component had a multitude of impact craters, what is the actual effect on the vehicle? If that impacted area were to be impacted again, how would the performance of the metal be affected? This study focuses on understanding the change in performance of CR4 mild steel in a multi-impact event from a spherical projectile.

Method and materials

A single stage gas gun was used to launch the projectile at the desired velocity at the target, using the Explosive Low Velocity Impact System (ELVIS).

ELVIS (figure 1) has a 22.3 mm diameter barrel which is 1.5 m in length and operates by using high pressure gas (either helium or air) to accelerate the projectile into the target material. Velocity measurements were taken using two light gates which use an oscilloscope (Tektronic TBS1104 four channel digital oscilloscope with a 100 mhz range and a maximum sampling rate of 1 GS s^{-1}) facilitate the recording of the impact velocity. A high-speed camera (Phantom v1212 operating at a frame rate of 12,600 frames/second) was used as a method to measure both the impact velocity and the residual velocity after perforation (further details provided in section).

The mass of each projectile, sabot and the plasticine were weighed prior to firing. The infra-red light gates provided the impact velocity (v_{impact}) and velocity in (v_{in}) and the high speed camera footage was used to measure v_{in} and velocity out (v_{out}) during a perforation shot (figure 2).

The projectile used in this study was a 10 mm G100 chrome steel spheres, manufactured with a tolerance of 5 μm, and a Vickers hardness of 700 HV [25]. Chrome ball bearings were selected for their high hardness compared to the target material to avoid projectile deformation during impact [17, 18]. The projectile was secured with plasticine within a cylindrical (domed) spilt sabots. The sabot provides sufficient obturation to facilitate a constant muzzle velocity at impact but was arrested by the sabot stripper to minimise the impact effect on the target material. A total of 57 experiments were conducted where full details of the shots are given in appendix A.

Prior to the testing, both the perforation velocity and the base level performance of the target material (3 mm CR4 Mild Steel (MS)) had to be determined. This target material was chosen as CR4 mild steel as it is a common sheet steel made to standard thicknesses. This enables consistent experimental results to be obtained. Additionally, CR4 mild steel was selected due to its comparable strength properties to Rolled Homogenous Armour (RHA) [26]. Furthermore, CR4 is easier to procure compared to RHA, thus making it a viable choice for target material without compromising on the expected material response. Using calibration targets of dimensions 75 $\times$ 75 mm, the perforation velocity was found by altering the impact velocity until perforation was achieved at a value of 435 m s^{-1}. Interestingly, at this velocity, the projectile both perforated and embedded in the target (with plug ejection), suggesting 435 m s^{-1} is at boundary of the perforation velocity of the target. To ensure reliable perforation, throughout this study, all perforation testing was conducted at 455 m s^{-1}.

To understand how an impact affects the ballistic properties of the 3 mm CR4 MS, its base level performance needed to be defined by experimentally measuring the impact and exit velocity of the projectile during a

Table 1. Materials and corresponding equation of State (EOS), Strength, and Erosion models chosen for simulation study of multi-hit capability of mild steel.

Function	Material	EOS	Strength	Erosion	Reference
Target	Steel 1006	Shock	Johnson Cook	Plastic Strain (1.05)	[27, 28]
Projectile	SS 304	Shock	Steinberg Guinan	—	[29]

Table 2. Fidelity study results of simulation to measure multi-hit capability of mild steel.

Mesh size (mm)	Projectile nodes	Target nodes	Total nodes	Time (min)
0.5	8,000	135,000	143,000	297
1	1,331	2,3104	24,435	52
2	216	2,888	3,104	5

perforating shot. The known velocities could then be converted to kinetic energy (KE), with the difference between KE_{in} and KE_{out} indicating amount of energy that the target material absorbed during perforation. Once the base level behaviour for the target material was determined, it can be compared to the energy absorbed by the target that has had a previous non-perforating impact.

Multi-hit testing

To replicate a non-perforated impact, targets were impacted at velocities between 40%–95% (164 to 425 m s^{-1}) of the perforation velocity, resulting in a spherical crater of depth x mm. The crater depth was defined as the distance between the deepest point of the crater and the level surface of the plate. For each impact, peak depth was measured using non-destructive techniques (height gauge (Heidenhain Length Gauge) & surface profiler (OSP100, Optical Surface Profiler, Uniscan Instruments)). Vickers hardness tests were used to understand how the impact was affecting the material across the impact crater, the details of which are given in appendix B.

The non-perforated crater was then impacted once more at perforation velocity (figure 2). To enable comparison between single and multi-hit targets, energy absorbed by the material was calculated for every non-perforating impact and compared against the base level performance.

Hardness tests

Samples were prepared from the single non-perforating impact craters samples and were cut to approximately 25 × 5 mm long samples to accommodate the hardness test machine (Highwood HWDM—7 microhardness tester) size limit (figure 3). Nonetheless these dimensions permit the capture of the crater and a given length from the impact event to study any local changes to the 3 mm CR4 MS targets.

A series of Vickers hardness tests were completed along the length of the sample approximately 10 microns below the impact surface as this was the closest measurement that could reliably be taken to the impact surface (see appendix B). The aim of these test was to understand the hardening effect that was taking place at the impact area and gain an understanding of the affected area surrounding the crater. Base line measurements were taken to determine a non-impacted sample hardness, three readings were taken and averaged, the base line hardness was found to be 165 HV.

Computer modelling of multi-hit testing

Ansys Autodyn 2020R2 was used to replicate and validate the experimental results (Dell G7; Intel i7 processor 2.20 GHz; 16 GB RAM). The use of computer modelling provided insight into the target response during the impact event and allowed the verification of the observations made during experiments. Table 1 shows the details of the materials and models used for the simulation study (table C1 contains details of the input parameters for the material models).

A fidelity study was conducted to optimise the computation time for the simulation, without compromising accuracy. The Lagrange solver was being used for this study because the model involved the interaction of two solid materials. The fidelity study was done to optimise the mesh size for the projectile and the target plate. Table 2 shows the results of the fidelity study.

From the fidelity study, it was observed that the model with 0.5 mm mesh had the highest accuracy but it was also computationally expensive. While the 0.5 mm mesh and 1 mm mesh showed similar deformation (~3.5 mm), the petalling was more detailed in the 0.5 mm mesh, making it the preferred choice. The 2 mm mesh was

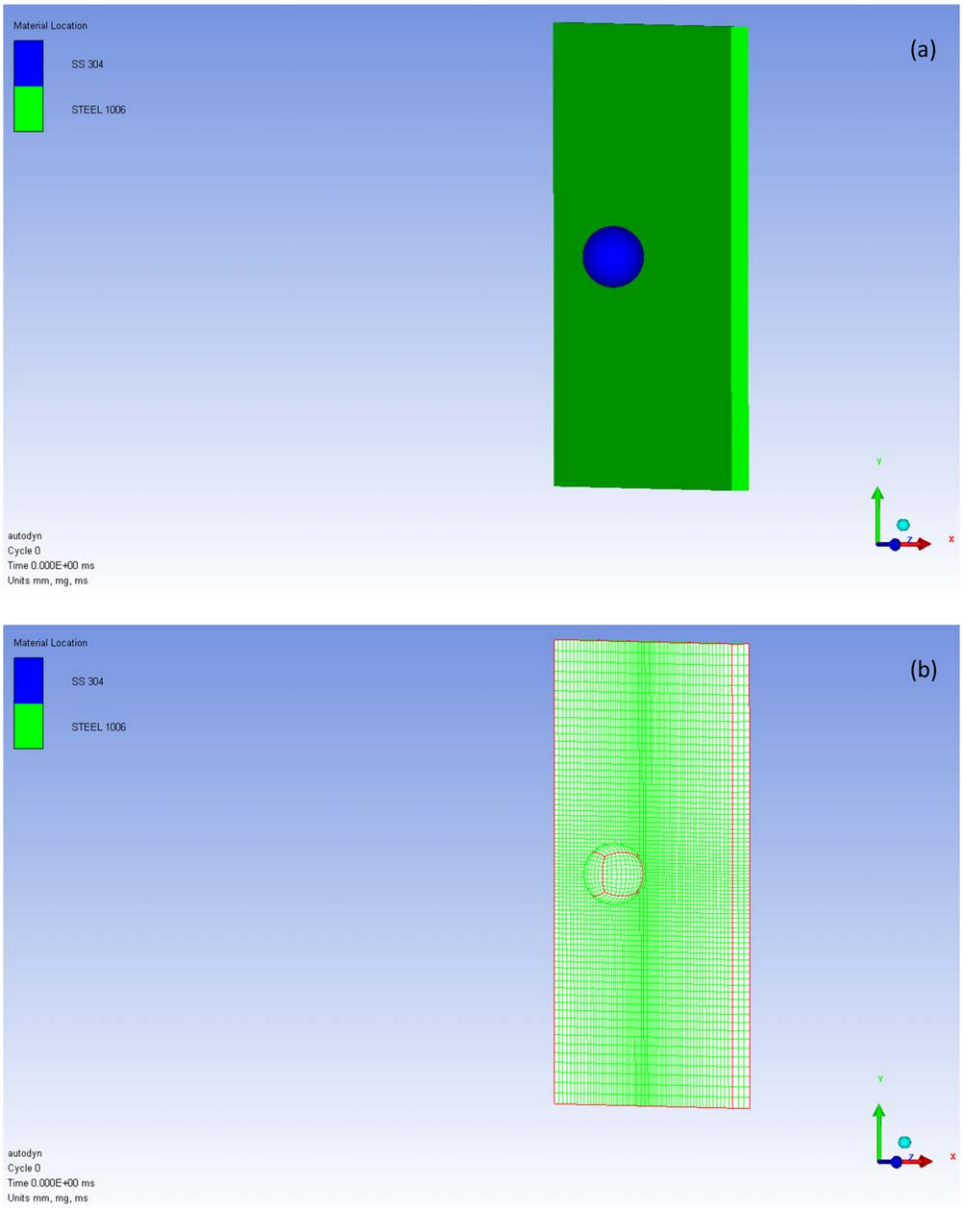


Figure 4. 3D simulation setup for impact of SS304 projectile (Blue; diameter: 10 mm) into Steel 1006 plate (Green; Dimensions: 3 mm × 75 mm × 75 mm) with (a) material location view; and (b) grid view with graded zoning at the point of impact.

Table 3. Crater depth measurements for mild steel plates subject to single impact from chrome steel projectile at varying velocities.

Impact velocity (m/s)	Critical crater depth (mm)
164	1.81
208	2.88
229	3.65
282	4.48
333	6.00
364	6.75
377	7.58
425	8.99

not selected because it was too coarse and had a larger error in deformation compared to the other two meshes. To achieve the required accuracy, and reduce computation time, a 1 mm mesh with central graded zoning of 0.5 mm was used. The mesh of the projectile was set at 0.5 mm to increase the accuracy of simulation. Figure 4 shows the 3D model setup with graded zoning over the area of impact.

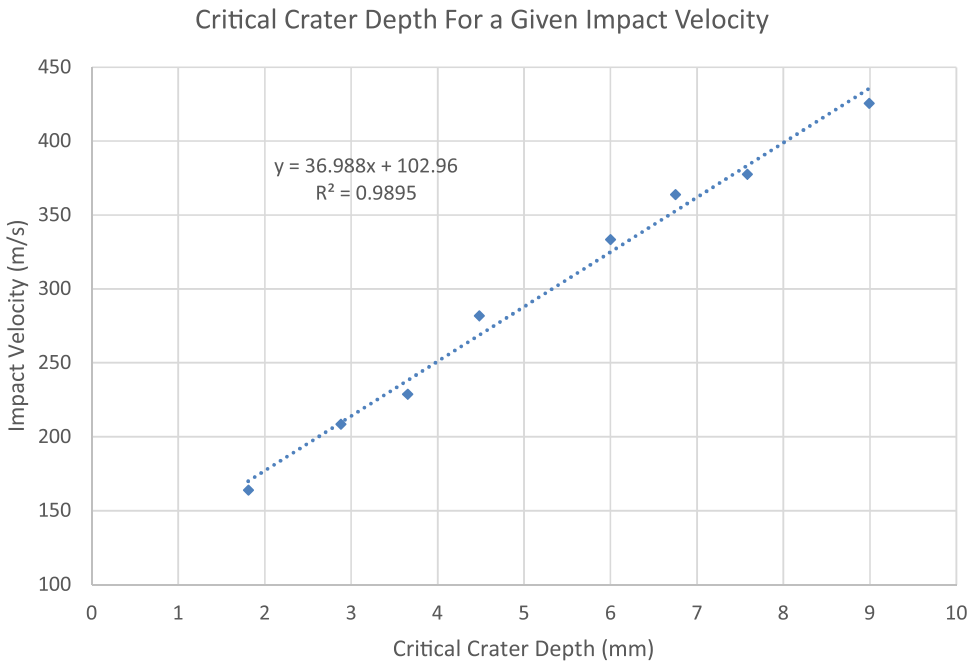


Figure 5. Critical crater depths for 3 mm thick mild steel plates subject to single impact from chrome steel projectile (diameter: 10 mm) at various non-perforating velocities.

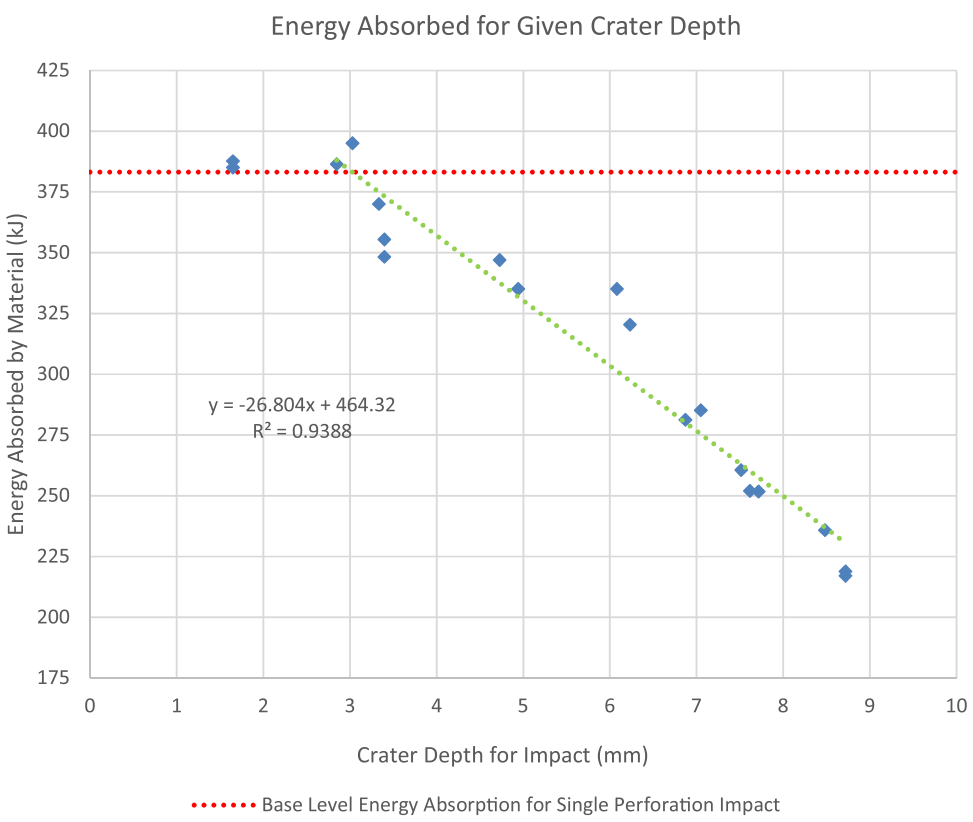


Figure 6. Energy absorbed by 3 mm thick mild steel plates subject to multiple impacts from a chrome steel projectile (diameter: 10 mm) at as a function of crater depth due to impact from first, non-perforating velocity impact.

Results and discussion

Eight targets were subject to an initial physical impact, each target was impacted with a different velocity (between 164–425 m s^{-1}) below the pre-determined perforation velocity, where the resultant crater depths were

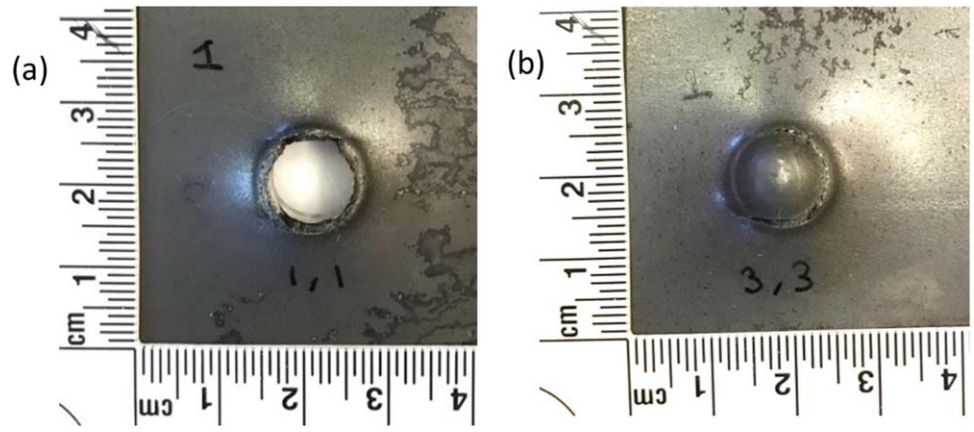


Figure 7. Failure mechanisms of 3 mm mild steel plate when subject to single impact by 10 mm spherical chrome steel projectile with impact velocity (a) 460 m s^{-1} (perforation); and (b) 430 m s^{-1} (non-perforation).

recorded (table 3). When plotted (figure 5), a positive linear relationship between increasing impact velocity and critical crater depth was found and thus can therefore be used to predict the critical crater depth for a given impact velocity. The critical crater depth is defined as the depth of crater required to affect the material's ability to absorb energy—a metric to measure the material's performance under impact loading conditions.

Multi-hit results

To establish a constant baseline the lowest kinetic energy required to achieve perforation in the mm CR4 mild steel was determined and calculated to be 383 kJ and represented by a dashed red line in figure 6. This baseline experiment was repeated three times to ensure statistical accuracy. The multi hit experiment was set up such that each target was impacted a second time with a projectile of the same size and mass. Figure 6 shows the energy absorbed by each secondary non-perforating impact velocity vs critical crater depth.

By taking the energy absorbed value as a percentage of the baseline performance, the reduction in material energy absorption could be calculated. The baseline energy absorption (red line) and the linear relationship (green line) intersect at the 3 mm crater depth, indicating crater depths up to 3 mm show no loss in ability to absorb energy. This transition point is coincidently the same as the material thickness, however the relevancy of this observation is currently unknown.

This study had a maximum non-perforating impact velocity of 425 m s^{-1} which resulted in the highest critical crater depth of 8.5 mm; this was approximately 10 m/s lower than the experimentally determined perforation velocity. This was limited due to the operational control at the top end of ELVIS's capabilities. It can be seen that there is a linear relationship between the crater depths of the first impact between 3–8.5 mm to the percentage reduction in the materials ability to absorb energy, with an R^2 value of 0.94. This combined with replication of data gives high confidence in this relationship.

For craters depths up to 3 mm the material behaves differently. The energy absorbed by the material increases by ~2% as the crater depth increases to 3 mm point. It is beyond that point the material starts to lose its absorption ability. The data set and examined samples show that once a crater depth of 8.5 mm is formed from an impact, the material has lost ~40% of its performance. The linear relationship determined from the data in this region predicts the residual performance of the material for a given impact crater. It suggests that for every millimetre the crater depth grows beyond 3 mm there is ~7% loss in performance.

Damage mechanisms

The various failure mechanisms for the impact experiments are shown in figures 7 to 11. For the perforating baseline impacts, high speed video showed plugging failure where the plug ejected above the residual velocity of the projectile as perforation occurs [24]. Furthermore, it can be observed that for the single perforating impact there is a correlation between the peak hardness value and where the target material failed just inside the crater lip. This matched the observed plugging failure for these single perforating impact experiments thus giving further confidence in the hardness test results. Conversely the failure modes for the multi-impact experiments varied between plugging (figure 8), petalling (figure 9) and a mixture of the two (figure 10). In addition to the failure modes in and around the craters, it was also noted that the deformation of the plate was a result of plastic failure.

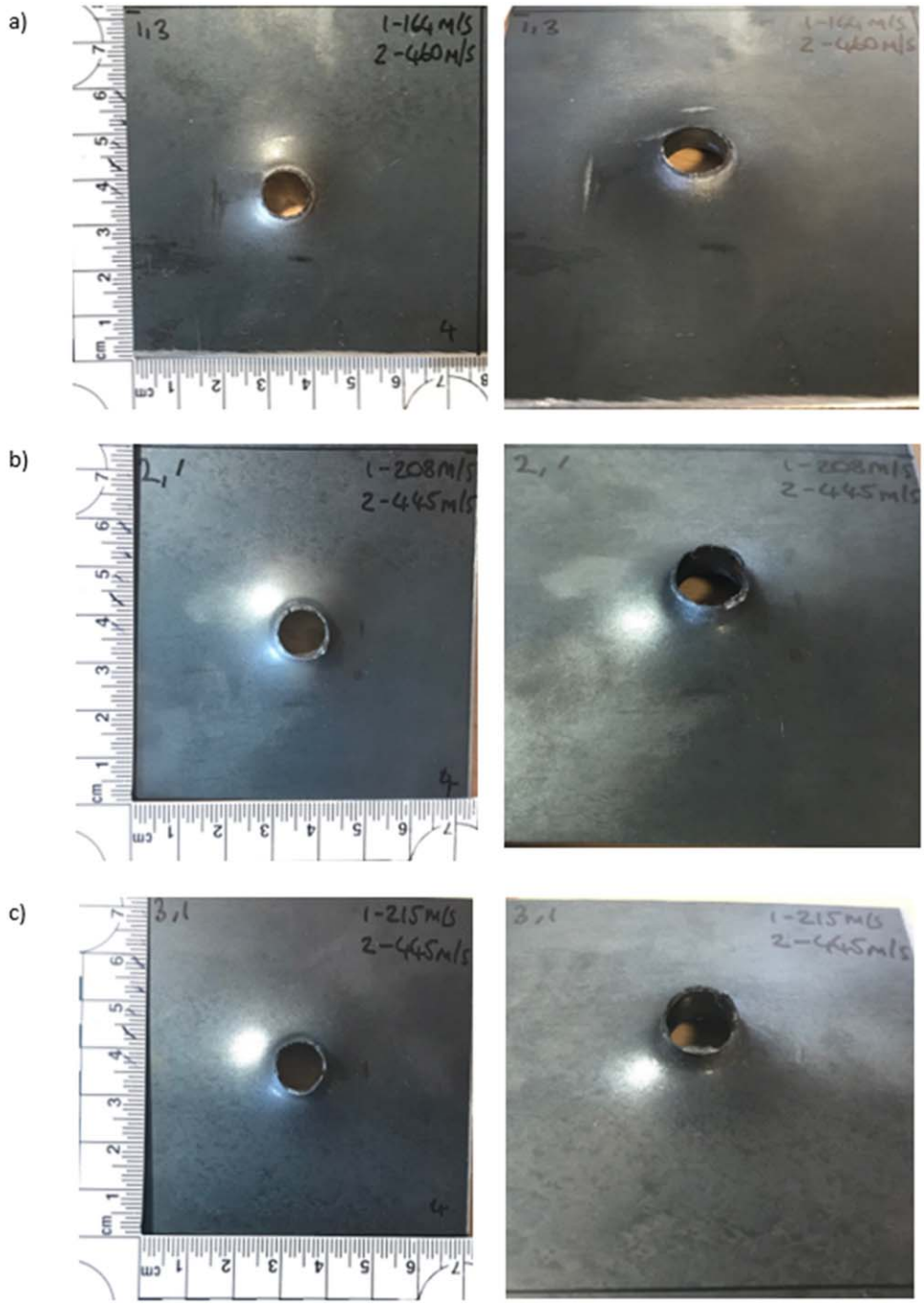


Figure 8. Failure mechanisms when 3 mm mild steel plate is subject to multi-impact experiments by 10 mm spherical chrome steel projectile; where initial impact velocities were (a) 164 m s^{-1}; (b) 208 m s^{-1}; and (c) 215 m s^{-1}.

Initial observations between the multi-impact experiments to the single perforating impact experiments is an increased amount of necking that is experienced before failure occurs. The increased necking is more representative of a hemispherical projectile failure as found by Landkof and Goldsmith [8] and Kpenyigaba *et al* [22]. It is speculated that the increased necking observed is due to the multiple impacts and localised effects inducing strain hardening enabling a potential cumulative necking effect before failure occurs. This is further supported by figure 11 which shows a sample which had a first impact of 165 m/s followed by a subsequent impact at 435 m s^{-1}. We would expect for a single impact of 435 m s^{-1} to achieve perforation (as this is the experimentally defined perforation velocity observed within this study), but in the instance where a previous impact of 165 m/s had occurred, this was not the case. The material has experienced increased necking in comparison to a single impact at 430 m s^{-1} (figure 7(b)) but did not perforate. The work hardening and thus the expected increase in strength (as found in Hall's investigation of work hardening [30]) would explain why the

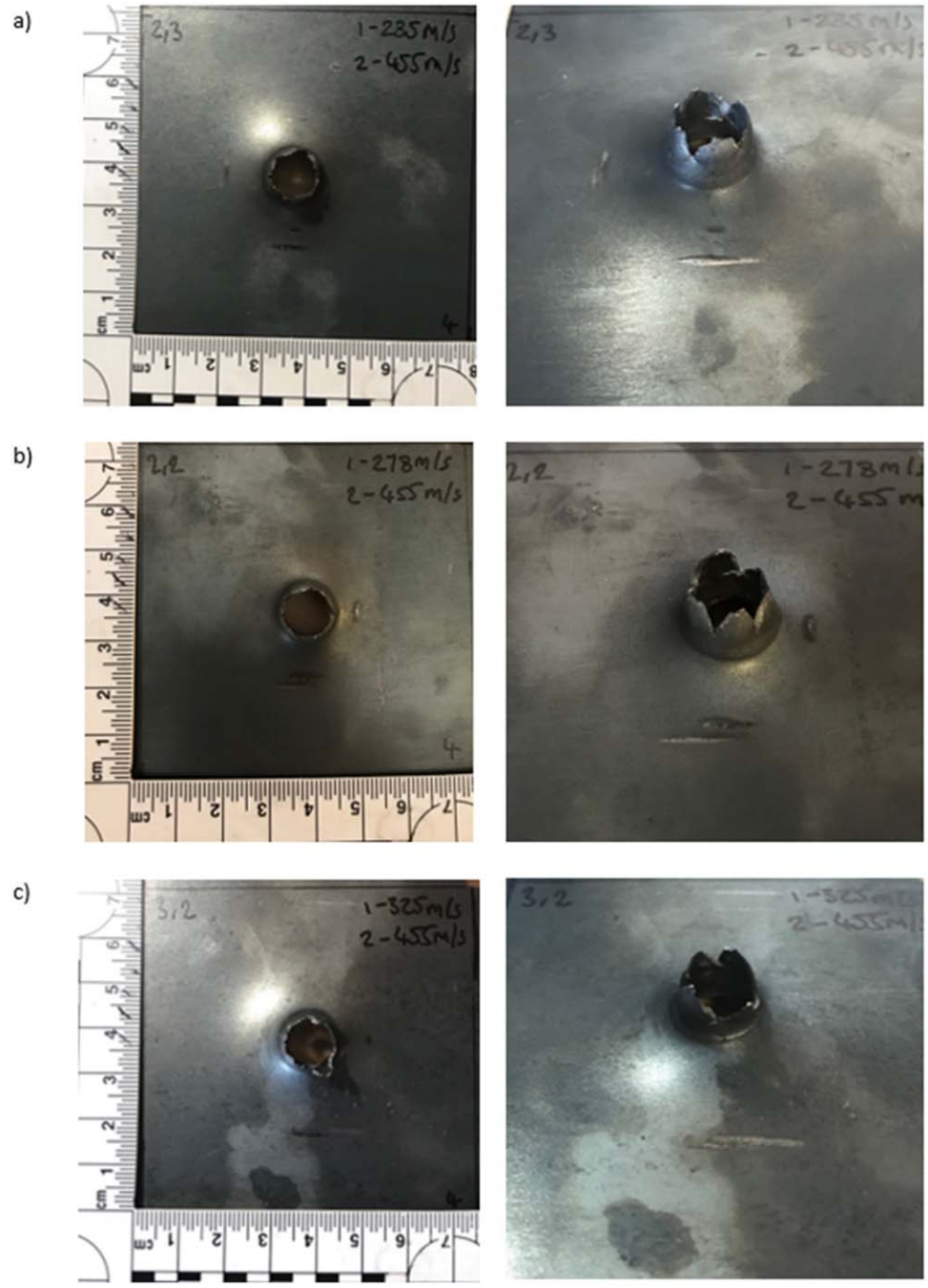


Figure 9. Failure mechanisms when 3 mm mild steel plate is subject to multi-impact experiments by 10 mm spherical chrome steel projectile; where initial impact velocities were (a) 285 m s^{-1}; (b) 278 m s^{-1}; and (c) 325 m s^{-1}.

435 m s^{-1} shot did not perforate in this instance. Investigating this phenomenon would form the basis for further study.

In figure 8, increased necking is observed however, plugging is still the failure mode of the target material. As the velocity of the initial impact increases this does not remain the case. Firstly, the hardness of the target increases at the impact location (See appendix B), resulting in work hardening at the impact location. It is shown in literature that a hardened target material would result in increased likelihood of petalling failure mode as shown in work completed by Wilkins and Goldsmith [9, 15, 16]. This work, relating the hardness to the failure mode is supported by examination of the impacted samples, which demonstrate petalling becoming the dominant failure mode as the non-perforating impact velocity increases.

Secondly as the impact velocity increases, and the critical crater depth increases, this results in a thinner cross section of material from the bottom of the crater to the back of the target. Thus, the effective thickness of the material is decreasing as the impact velocity increases. Previous work from Wilkins [15] and Wierzbichi [6], for single impact scenarios, shows that as the target behaves as a thinner plate, petalling becomes the more dominant

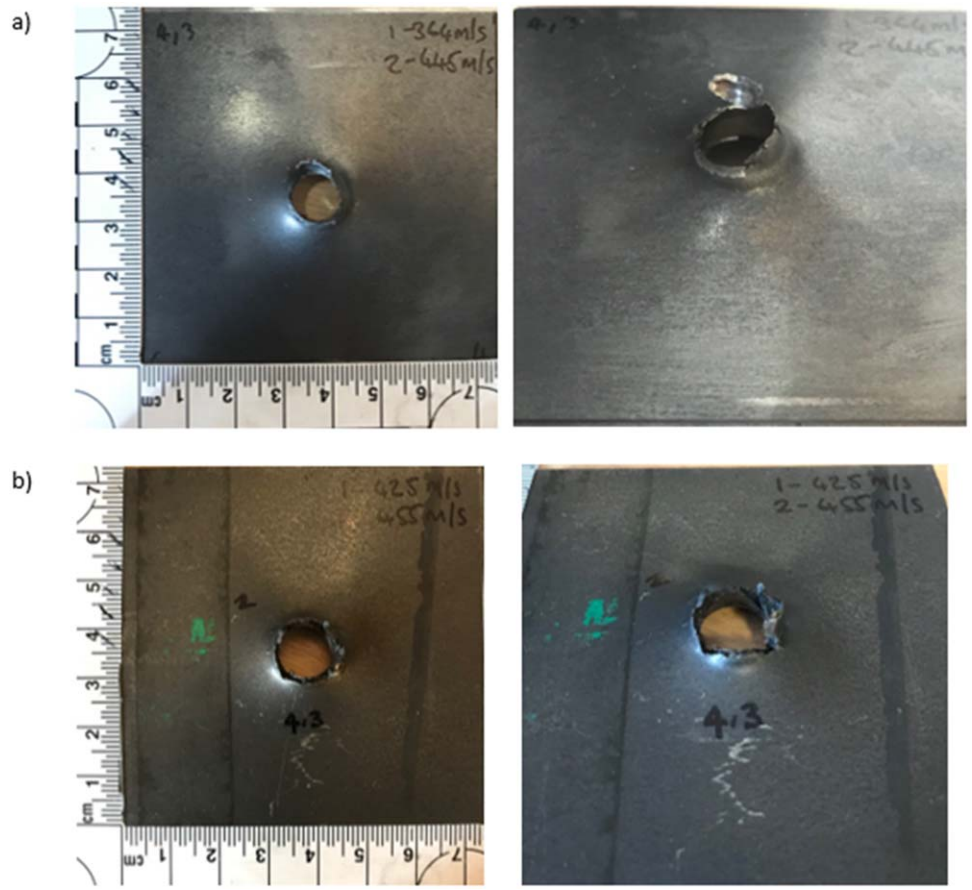


Figure 10. Failure mechanisms when 3 mm mild steel plate is subject to multi-impact experiments by 10 mm spherical chrome steel projectile; where initial impact velocities were (a) 364 m s^{-1}; and (b) 425 m s^{-1}.

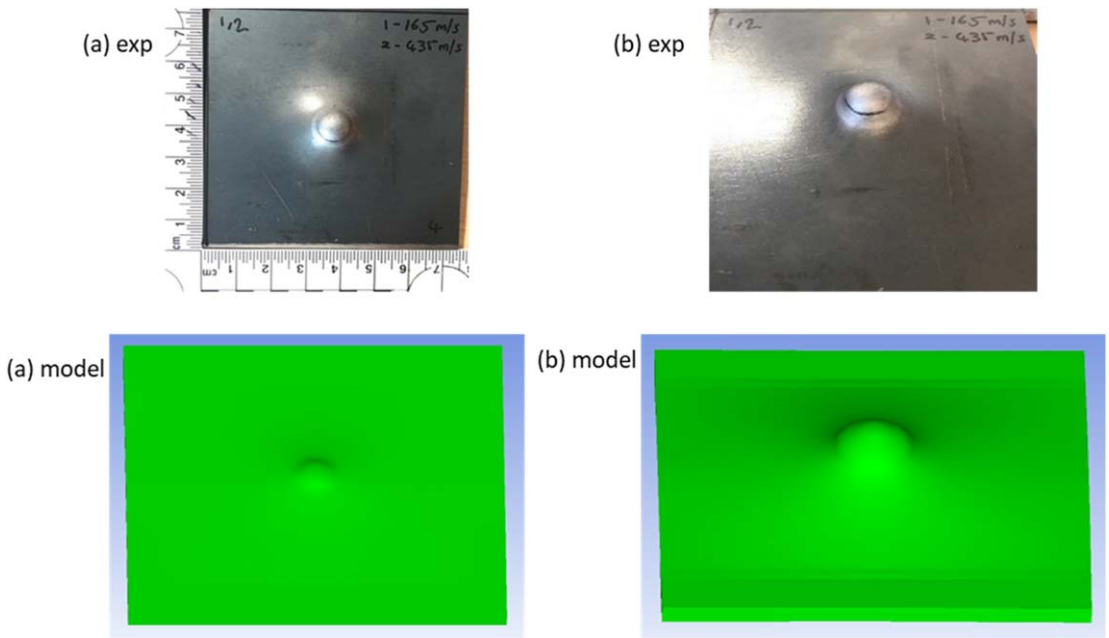


Figure 11. Failure mechanisms when mild steel plate is subject to multi-impact (experiments results shown above and simulation results shown below) by 10 mm spherical chrome steel projectile; where initial impact velocities were (a) 165 m s^{-1}; and second impact velocity of (b) 435 m s^{-1}.

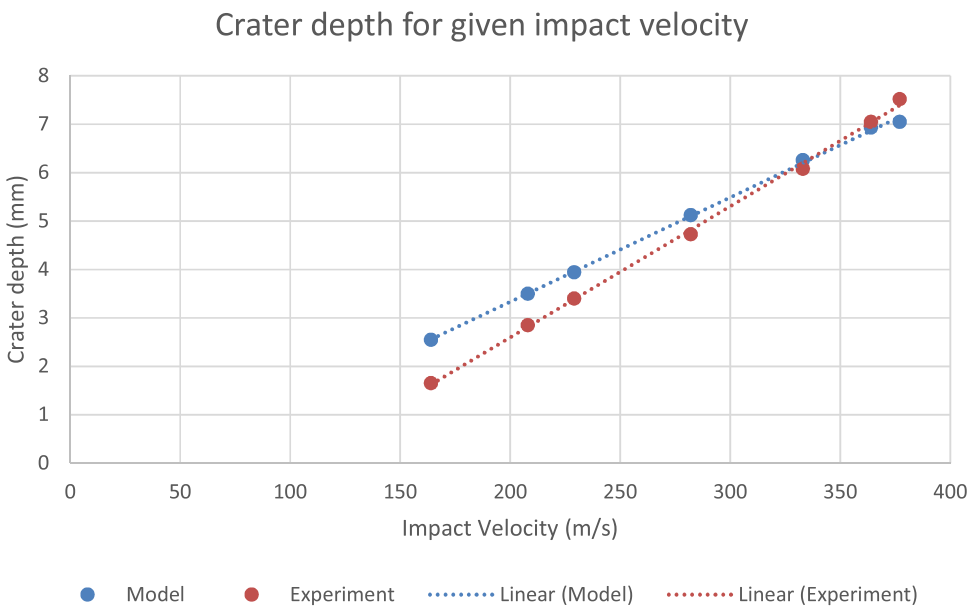


Figure 12. Comparison of model and experimental data for crater depth as a function of impact velocity when mild steel plate is subject to non-perforating impact from spherical chrome steel projectile.

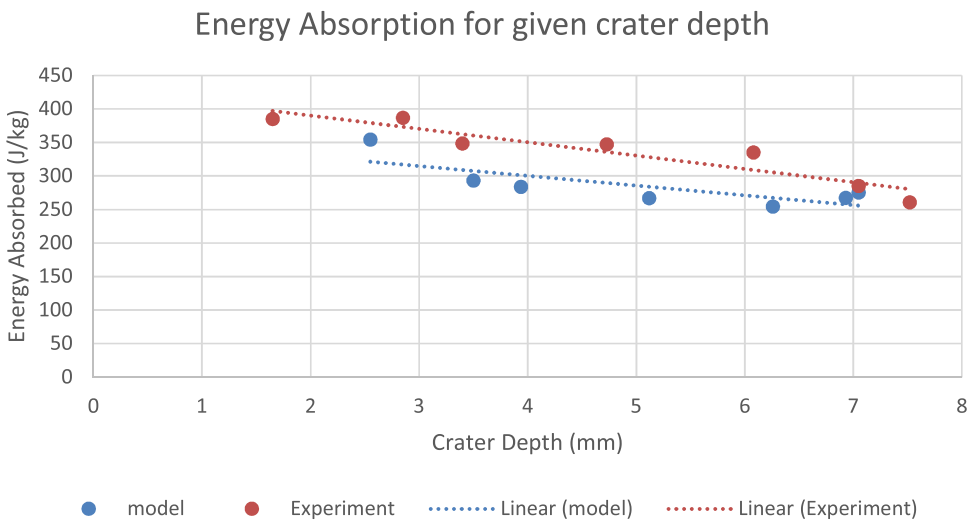


Figure 13. Comparison of model and experimental data for energy absorption as a function of crater depth when mild steel plate is subject to multiple impacts from spherical chrome steel projectile.

failure mode. This theory discussed by Wilkins and Wierzbichi directly links with the experienced failure modes in a multi-impact scenario despite it not being directly investigated. As a combination of both work hardening and the effective material thickness reducing, the failure mechanism transitions from plugging to petalling. The transition of failure mode from plugging to petalling occurs in samples beyond the 3 mm critical crater depth, relating this back to the target thickness. Again, demonstrating how crucial the target thickness is for identifying the most likely failure mode, investigating this relationship to other target thicknesses will be the basis for further study. These results would suggest that an impact at a sufficient velocity to impart a crater at a depth deeper than the initial thickness of the target material, caused in part by the increase in necking in the target, results in a change of failure mechanism for a subsequent perforating impact (multi hit). This change in failure mechanism, could be why the material starts to lose performance and hence the decrease in impact energy absorption from that critical crater depth onwards.

In some rare instances, a multi-impacted target (figure 11) did not perforate. Single impact failure modes were thoroughly investigated in available literature [7, 16, 24] it was found that plugging was the most common failure mode. Although valuable research, these results did not provide insight into how the material may fail in a

multi-impact scenario other than for the use of comparison, thus figure 11 shows a response that was not included in the main plotted data.

Simulation results

The simulations were compared to the experiments based on crater depth against impact velocity (figure 12), and energy absorption against crater depth (figure 13). The simulation results showed a similar trend in data with respect to the experiment results.

Based on the crater depth comparisons, it was observed that the model predicted increased crater depth than what was measured experimentally up until ~350 m s^{-1} at which point it transitions to a slight under prediction. One of the possible reasons for this is that the model is representative of ideal conditions and does not account for the errors in the experimental process. Here, experimental errors refer to errors in measurement and prediction of crater depth using the trend line equation from figure 6. The shock EOS is used for solid bodies to measure the response to shock and pressure for a given thermodynamic state. In the case of multiple impacts, the thermodynamic state of the target changes slightly between impacts, which creates a gap between the simulation and experimental data.

The experiment measured energy absorption of the plate by the change in kinetic energy of the projectile, under the assumption that all the energy lost by the projectile is absorbed by the plate. The computational model uses the EOS and strength model of the plate material to measure the change in internal energy of the plate. Additionally, empirical observation of the models shows localised stress formation in and around the crater after the first impact which is unable to be included in the computational model due to limitations of the modelling software. The localised stress formation influences the mechanical properties of the material and can be supported by the experimental hardness data (See appendix B). The localised stress formation around the crater suggests work hardening of the material during the impact event. The plastic deformation, and eventual failure of the material when subject to multiple impacts further validates the observation of the reduction in material hardness inside the crater after the first non-perforating impact. The difference in methods for measuring energy change results in the difference in measured values for energy absorption of the plate. Although there is a difference in values of energy absorbed, both cases show a general downward trend in energy absorption as the crater depth increases. The increased deformation during the first non-perforating impact implies increased energy absorption, thus reducing the material's ability to absorb energy during the second impact. This results in the failure of the target material and the ejection of a fragment as the projectile perforates the plate. Additionally, the experimental method does not account for the energy loss from the plate to the fragment that is released during perforation. Consequently, this creates a source of error in the estimation of energy absorbed by the plate during the impact event and supports the deviation in results between the experimentally and computationally derived responses.

Conclusions

An experimental program consisting of 57 shots using a 10 mm stainless steel ball bearing projectile against 3 mm CR4 MS plate to determine how singular and multi-impacts affect the materials failure models and energy absorption was conducted. Hardness tests were completed to support the experimental findings, and computational modelling was conducted to aid in understanding the effects the impact had on the target material. The main conclusions are as follows:

1. The data produced showed that the 3 mm CR4 MS did not lose any ability to absorb energy when subject to a prior single impact resulting in a crater 3 mm or less. Subsequent perforation shots within this range resulted in plugging failure.
2. With an increase in impact velocity for the non-perforating impact there was a linear relationship between the depth of crater to reduction in absorption ability.
3. A reduction in the materials' energy absorption ability by ~7% per mm of crater depth from 3.0 mm to 8.5 mm was observed. Within this range the subsequent perforation shot results in a petalling failure.
4. This results in an overall conclusion that craters with a depth equal to or less than the material thickness, has no effect on the materials ability to absorb energy.

These results are crucial to understand how a singular non-perforating impact has affected a target material and demonstrates that it is possible to understand the residual multi-impact performance of the material for a given impact and thus enabling a threshold to be set for an acceptable loss of performance during damage assessments. This study provides empirical evidence to inform engineers during damage assessments for armour

systems and therefore provide scientific evidence for an informed risk assessment to be conducted of the materials post impact. Future work based on this study looks to focus on verifying these findings in other armour grade materials; and understand the effect of different sizes and shapes of projectiles on the transition from energy absorption to failure.

Acknowledgments

The author would like to thank Mr Andrew Roberts and Mr David Miller for their advice, supervision, and assistance throughout this research. Further thanks to Mr Adrian Mustey and Mr Karl Norris for their guidance and support in materials preparation and evaluation.

Data availability statement

All data that support the findings of this study are included within the article (and any supplementary files).

Appendix A: Additional shot information

Table A1. Detailed firing information.

						Mass (g)				
Shot #	Plate #	Reference square	Gas pressure (He)(bar)	△t (s)	Velocity IN (Light Gates)	Projectile	Sabot	Total	KE Impact (kJ)	Perforate?
1	1	1, 1	50	87	459.77	4.1	3.3	7.4	433.35	Yes
2	1	1, 2	30	106	377.36	4.1	3.2	7.3	291.92	No
3	1	1, 3	40	91	439.56	4.1	3.2	7.4	396.09	Yes
4	1	2, 1	35	99	404.04	4.1	3.2	7.3	334.66	No
5	1	2, 2	38	94	425.53	4.1	3.2	7.4	371.21	No
6	1	2, 3	39	94	425.53	4.1	3.2	7.4	371.21	No
7	1	3, 1	39	92	434.78	4.1	3.2	7.4	387.52	Yes
8	1	3, 2	40	94	425.53	4	3.2	7.4	362.15	Yes
9	1	3, 3	—	—	—	4.1	3.2	7.4	—	No
10	2	1, 1	42	90	444.44	4.1	3.3	7.4	404.94	Yes
11	2	1, 2	42	89	449.44	4.1	3.3	7.4	414.09	Yes
12	2	1, 3	42	88	454.55	4.1	3.2	7.3	423.55	Yes
33	4	1, 2	5	244	163.93	4.074	3.2218	7.4249	54.74	No
34	4		41	92	434.78	4.0737	3.2302	7.4352	385.04	No
35	4	1, 3	5	244	163.93	4.0761	3.2155	7.4566	54.77	No
36	4		41	86	465.12	4.0742	3.2277	7.4216	440.69	Yes
37	4	1, 4	5	244	163.93	4.0758	3.2222	7.4213	54.77	No
48	4	1, 1	8	192	208.33	4.0739	3.2344	7.4389	88.41	No
49	4	2, 1	8	192	208.33	4.0737	3.2426	7.4466	88.40	No
50	4		41	90	444.44	4.0765	3.258	7.4425	402.62	Yes
51	4	3, 1	8	186	215.05	4.0756	3.2582	7.4583	94.24	No
52	4		41	90	444.44	4.0755	3.2557	7.4592	402.52	Yes
19	2	2, 1	10	175	228.57	4.1	3.2	7.4	107.10	No
20	2		42	93	430.11	4.1	3.2	7.4	379.23	Yes
21	2	2, 2	10	175	228.57	4.1	3.2	7.4	107.10	No
22	2		42	92	434.78	4.1	3.2	7.4	387.52	Yes
23	2	2, 3	10	179	223.46	4.1	3.2	7.4	102.37	No
24	2		42	91	439.56	4.0	3.3	7.4	386.43	Yes
25	2	2, 4	10	175	228.57	4.1	3.2	7.4	107.10	No
38	4	2, 2	15	144	277.78	4.0756	3.2254	7.411	157.24	No
39	4		41	88	454.55	4.0748	3.2145	7.3775	420.95	Yes
40	4	2, 3	15	140	285.71	4.0744	3.2369	7.4256	166.30	No
41	4		41	88	454.55	4.0748	3.2321	7.3905	420.95	Yes
42	4	2, 4	15	142	281.69	4.0769	3.2284	7.4146	161.75	No
43	4	3, 2	22	122	327.87	4.076	3.2315	7.4314	219.08	No
44	4		42	88	454.55	4.0751	3.2296	7.4201	420.98	Yes

Table A1. (Continued.)

Shot #	Plate #	Reference square	Gas pressure (He)(bar)	Δt (s)	Velocity IN (Light Gates)	Mass (g)			KE Impact (kJ)	Perforate?
						Projectile	Sabot	Total		
45	4	3, 3	22	120	333.33	4.077	3.2225	7.4125	226.50	No
46	4		42	86	465.12	4.0743	3.2267	7.4271	440.70	Yes
47	4	3, 4	22	120	333.33	4.0759	3.2431	7.4464	226.44	No
53	4	4, 1	25	110	363.64	4.0762	3.2401	7.454	269.50	No
54	4	4, 2	25	112	357.14	4.0762	3.2345	7.477	259.96	No
55	4		41	90	444.44	4.0757	3.2413	7.411	402.54	Yes
56	4	4, 3	25	110	363.64	4.076	3.249	7.4105	269.49	No
57	4		41	90	444.44	4.0759	3.2383	7.4081	402.56	Yes
26	2	3, 1	30	104	384.62	4.1	3.2	7.4	303.25	No
27	2		42	89	449.44	4.1	3.2	7.4	414.09	Yes
28	2	3, 2	30	105	380.95	4.1	3.2	7.4	297.51	No
29	2		42	89	449.44	4.1	3.2	7.4	414.09	Yes
30	2	3, 3	30	103	388.35	4.1	3.2	7.4	309.17	No
31	2		42	89	449.44	4.1	3.2	7.4	414.09	Yes
32	2	3, 4	30	106	377.36	4.1	3.2	7.4	291.92	No
18	2	4, 1	38	94	425.53	4.1	3.2	7.4	371.21	No
19	2		42	88	454.55	4.1	3.2	7.4	423.55	Yes
15	2	4, 3	38	94	425.53	4.1	3.3	7.4	371.21	No
16	2		42	88	454.55	4.1	3.2	7.3	423.55	Yes
13	2	4, 4	38	96	416.67	4.1	3.2	7.4	355.90	No
14	2		42	88	454.55	4.1	3.2	7.4	423.55	Yes

Appendix B: Hardness testing

Figure B1 highlights the trend between the progressive increase in hardness as the impact velocity increases, with baseline hardness indicated by a dashed red line.

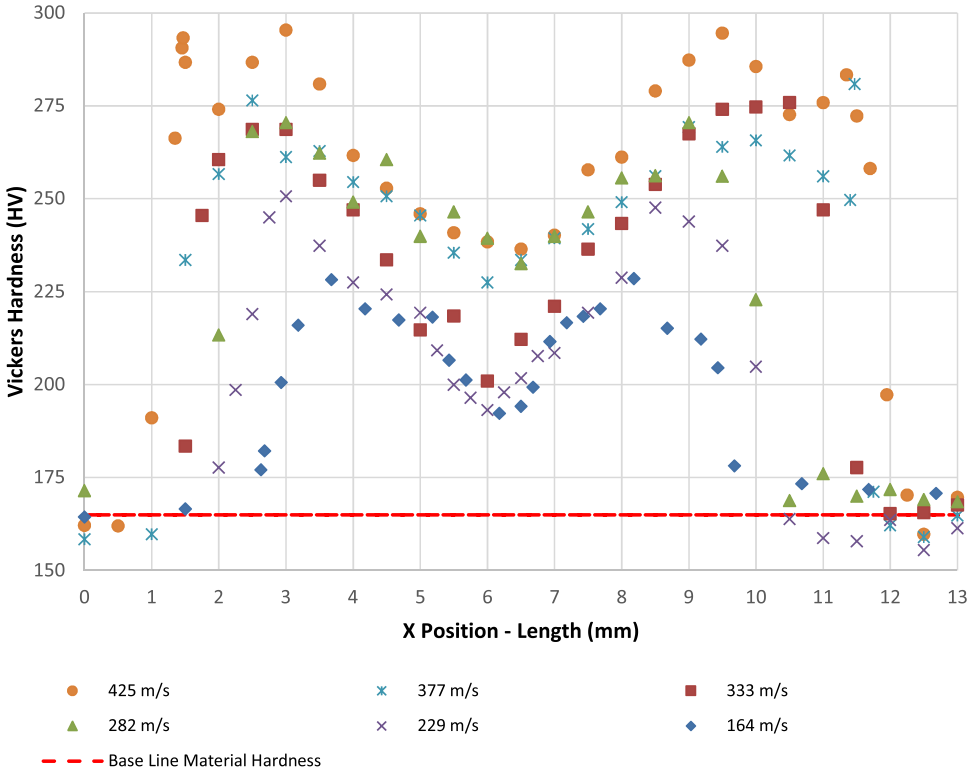


Figure B1. Vickers hardness of mild steel plate at different locations in crater after plate is subject to single non-perforating impact from chrome steel projectile at different velocities.

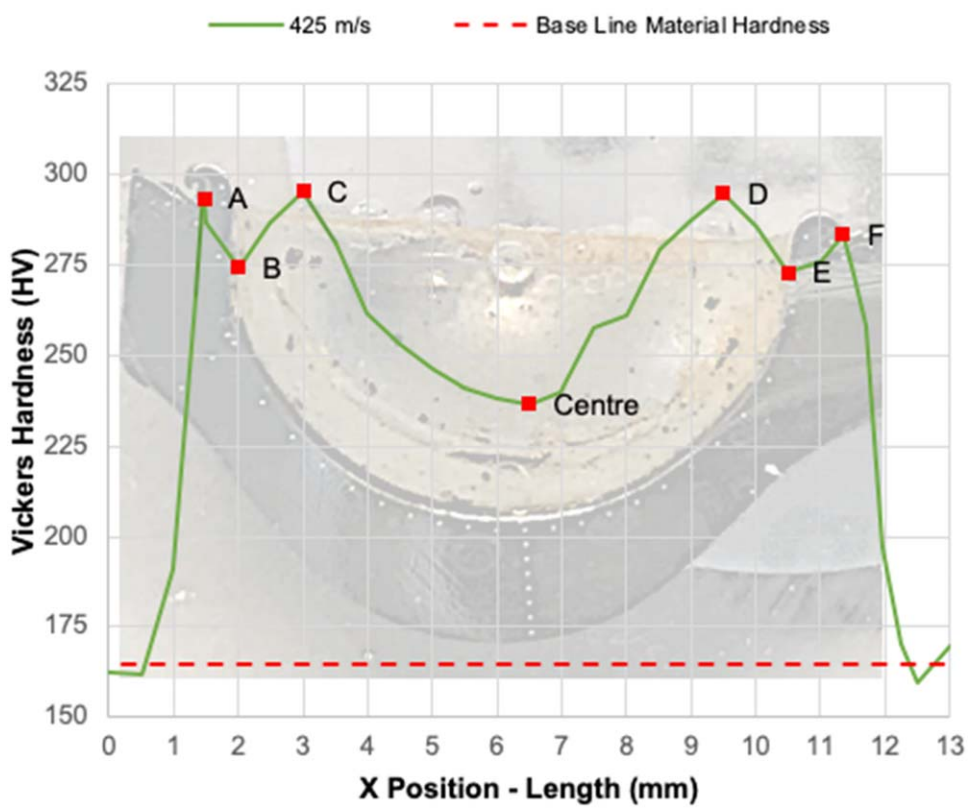


Figure B2. Vickers Hardness Measurements at various points inside mild steel plate crater subjected to non-perforating impact from chrome steel projectile with velocity 425 m s^{-1}.

Analysing the hardness plots for the 425 m s^{-1} impact crater, figure B2 overlays the impact crater and the hardness test results, although not a perfect overlay it gives a good understanding of where on the crater the hardness readings were obtained. There is a symmetrical trend across the crater which would be expected from a perpendicular spherical impact. It shows an abrupt increase from 'base-level' hardness (165 HV) to 290 HV at 1.5 mm (A), followed by a slight dip to 275 HV at 2 mm (B), to rise back to 287 HV at 3 mm (C). Almost identical values are found at 11.75 mm (D), 10.5 mm (E) and 9.5 mm (F) respectively.

This failure point in the crater strongly correlates to the peak hardness values described in figure B2 at point C and D, just inside the crater lip. The hardness tests show that the effect the impact has on the material is localised. It shows that for a perpendicular impact from a 10 mm chrome sphere, the hardening effects are minimal beyond the area of impact. In the instance of the highest measured impact velocity of 425 m s^{-1}, a change in hardness is measured over a 12 mm diameter. The hardness tests also highlighted the location of the peak hardness values along the crater.

Appendix C : Material model parameters

Table C1. Detailed material model input parameters.

Material	EOS	Strength	Erosion
Steel 1006	Shock	Johnson Cook	Plastic Strain
	Gruneisen coefficient: 2.17	Shear Modulus: 8.18×10^7 kPa	
	Parameter C1: 4.569×10^3 m s^{-1}	Yield Stress: 3.50×10^5 kPa	1.05
	Parameter S1: 1.49	Hardening Constant: 2.75×10^5 kPa	
	Parameter Quadratic S2: 0	Hardening Exponent: 0.36	
	Relative Volume, VE/V0: 0	Strain Rate Constant: 0.022	
	Relative Volume, VB/V0: 0	Thermal Softening Exponent: 1.00	
	Parameter C2: 0	Melting Temperature: 1.81×10^3 K	

Table C1. (Continued.)

Material	EOS	Strength	Erosion
	Parameter S2: 0	Ref. Strain Rate (/s): 1.00	
	Reference Temperature: 300 K	Strain Rate Correction: 1st Order	
	Specific heat: 452 J kgK^{-1}		
	Thermal conductivity: 0		
SS 304	Shock	Steinberg Guinan	N/A
	Gruneisen coefficient: 1.93	Shear Modulus: 7.70×10^7 kPa	
	Parameter C1: 4.57×10^3 m s^{-1}	Yield Stress: 3.40×10^5 kPa	
	Parameter S1: 1.49	Max Yield Stress: 2.50×10^6 kPa	
	Parameter Quadratic S2: 0	Hardening Constant: 43.00	
	Relative Volume, VE/V0: 0	Hardening Exponent: 0.35	
	Relative Volume, VB/V0: 0	Derivative dG/dP: 1.74	
	Parameter C2: 0	Derivative dG/dT: -3.504×10^4 kPa/K	
	Parameter S2: 0	Derivative dY/dP: 0.007684	
	Reference Temperature: 300 K	Melting Temperature: 2.38×10^3 K	
	Specific heat: 422.99 J kgK^{-1}		
	Thermal conductivity: 0		

Declaration of interests

The authors declare that they have no known competing financial interests or personal relationships that could have appeared to influence the work reported in this paper.

The authors declare the following financial interests/personal relationships which may be considered as potential competing interests:

ORCID iDs

B Thawani https://orcid.org/0000-0002-7179-2039
R Critchley https://orcid.org/0000-0001-5423-9859

References

[1] Zukas J A 1982 Penetration and perforation of solids *Impact Dynamics.* (Canada: Wiley) 155–214
[2] 2015 Cranfield University *Ammunition Technology Handbook - Warheads.* **1** 48
[3] Hazell P 2015 Metallic armour materials and structures *Armour: Materials, Theory, and Design.* 1st edn pp 177–206
[4] Doig A 1999 Why is most military hardware metallic? *Military Metallurgy.* (Shrivenham: IOM Communications) pp 20–1
[5] University IS. Nondestructive Evaluation Physics : Materials. 2021. Available at: https://nde-ed.org/Physics/Materials/Mechanical/Toughness.xhtml (Accessed: 7 January 2022)
[6] Wierzbicki T 1999 Petalling of plates under explosive and impact loading *Int. J. Impact Eng.* **22** 935–54
[7] Backman M E and Goldsmith W 1978 The mechanics of penetration of projectiles into targets *Int. J. Eng. Sci.* **16** 1–99
[8] Landkof B and Goldsmith W 1985 Petalling of thin, metallic plates during penetration by cylindro-conical projectiles *Int. J. Solids and Structures. Pergamon Press Ltd* **21** 245–66
[9] Goldsmith W, Liu T W and Chulay S 1965 Plate impact and perforation by projectiles *Exp. Mech.* **5** 385–404
[10] Rusinek A, Rodríguez-Martínez J A, Zaera R, Klepaczko J, Arias A and Sauvelet C 2009 Experimental and numerical study on the perforation process of mild steel sheets subjected to perpendicular impact by hemispherical projectiles *Int. J. Impact Eng.* **36** 565–87
[11] Hazell P 2015 Penetration mechanics *Armour: Materials, Theory, and Design.* 1st edn pp 91–136
[12] Jones N and Paik J K 2012 Impact perforation of aluminium alloy plates *Int. J. Impact Engineering. Elsevier Ltd* **48** 46–53
[13] Corbett G G, Reid S and Johnson W 1996 Impact loading of plates and shells by free-flying projectiles: A review *Int. J. Impact Eng.* **18** 141–230
[14] Lenihan D, Ronan W, O'Donoghue P E and Leen S B 2019 A review of the integrity of metallic vehicle armour to projectile attack *Proc. Inst. Mech. Eng. Part L J. Mater. Des. Appl.* **233** 73–94
[15] Wilkins M L 1978 Mechanics of penetration and perforation *Int. J. Eng. Sci.* **16** 793–807
[16] Golsdmith W and Finnegan S A 1971 Penetration and perforation processes in metal targets at and above ballistic velocities *Int. J. Mech. Sci.* **13** 843–66
[17] Corran R S J, Shadbolt P J and Ruiz C 1983 Impact loading of plates - an experimental investigation *Int. J. Impact Eng.* **1** 3–22
[18] Neilson A J 1985 Empirical equations for the perforation of mild steel plates *Int. J. Impact Eng.* **3** 137–42
[19] Simonsen B C and Lauridsen L P 2000 Energy absorption and ductile failure in metal sheets under lateral indentation by a sphere *Int. J. Impact Eng.* **24** 1017–39
[20] Rusinek A 2009 Relation between strain hardening of steel and critical impact velocity in tension *J. Theoretical and Applied Mechanics.* **47** 645–65

[21] Rodríguez-Martínez J A, Rusinek A, Chevrier P, Bernier R and Arias A 2010 Temperature measurements on ES steel sheets subjected to perforation by hemispherical projectiles *Int. J. Impact Eng.* **37** 828–41
[22] Kpenyigba K M, Jankowiak T, Rusinek A and Pesci R 2013 Influence of projectile shape on dynamic behavior of steel sheet subjected to impact and perforation *Thin-Walled Structures. Elsevier* **65** 93–104
[23] Lynch N J and Pitcher P 2016 The influence of adjacent impact on the perforation of fragments
[24] Pradhan P K, Gupta N K, Ahmad S, Biswas P P and Dayanand 2017 Numerical investigations of spherical projectile impact on 4 mm thick mild steel plate *Procedia Engineering. Elsevier B.V.* **173** 109–15
[25] ATLAS BALL AND BEARING CO. LIMITED. CHROME STEEL BALL DATA SHEET. 2010
[26] Matmatch. ISO 3574 Grade CR4 - Material Data Sheet. 2022.
[27] Johnson Cook. Selected hugoniots: EOS. 7th international symposium on ballistics. 1969
[28] Standards B of I. IS 513 2008 Cold reduced low carbon steel sheets and strips [MTD 4: Wrought Steel Products]. New Delhi; 2008. Available at: www.bis.org.in
[29] Steinberg D 1996 Equation of state and strength properties of selected materials *Lawrence Livermore National Laboratory*
[30] Hall E O 1954 Variation of hardness of metals with grain size *Nature* 948–9



https://dspace.org/

Multi-impact response of CR4 mild steel: Characterising the transition from absorption to failure

Thawani, Bonny; Batchelor, T.; Painter, Jonathan; Hazael, Rachael; Critchley, Richard

2023-03
Institute of Physics (IOP)
https://doi.org/10.1088/2631-8695/acc0de
Thawani B, Batchelor T, Painter J, et al., (2023) Multi-impact response of CR4 mild steel: Characterising the transition from absorption to failure. Engineering Research Express, Volume 5, Issue 1, March 2023, Article number 015061

Downloaded from a DSpace repository. https://dspace.org/